Graphical Abstract

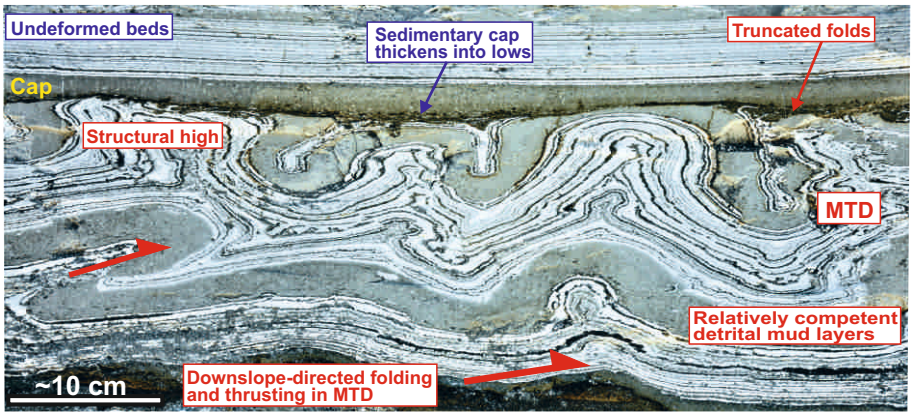

Identifying soft-sediment deformation in rocks

G.I. Alsop[1], R. Weinberger[2, 3], S. Marco[4], T. Levi[2].
1) Department of Geology and Petroleum Geology, School of Geosciences,
University of Aberdeen, Aberdeen, UK. (e-mail: Ian.Alsop@abdn.ac.uk)
2) Geological survey of Israel, Jerusalem, Israel.
3) Department of Geological and Environmental Sciences, Ben Gurion University of the Negev, Beer Sheva, Israel.
4) Department of Geophysics, School of Geosciences, Tel Aviv University, Israel.

Abstract

The correct identification of 'sedimentary' folds and fabrics created during gravity-driven deformation of unlithified successions from those 'tectonic' structures formed during regional deformation is essential when interpreting geological histories preserved within the rock record. This topic has become increasingly relevant over the past 40 years as improved seismic resolution and coverage have led to the realisation that significant portions of unlithified sediments along the continental margins undergo gravity-driven deformation to create mass transport deposits (MTD's). The late-Pleistocene Lisan Formation, exposed in the Dead Sea Basin, was chosen as a case study because it remains poorly lithified, and structures developed within it are unequivocally related to 'soft-sediment' deformation (SSD) created when the succession underwent downslope-directed movement. This work tests various assertions previously used to deduce if structures were formed in unlithified sediments or during 'hard-rock' deformation (HRD) associated with subsequent tectonism. Within the Lisan Formation, we describe veins developed along fractures, and cleavage forming axial-planar to folds, that are structures previously assumed to be restricted to HRD. In addition, truncated folds, incorporation of deformed fragile fragments into overlying sediment, and cross-cutting clastic dykes are all indicative of SSD. The key diagnostic feature in establishing SSD is the sedimentary infill of irregular erosive surfaces that truncate underlying structures. Although compaction and diagenesis have not played a significant role in the case study, caution should be exercised when examining structures preserved in the rock record as folds and fabrics originally created by SSD may be considerably enhanced and altered where significant overburden exists.

Keywords: soft-sediment deformation, mass transport deposit, Dead Sea

1. Introduction

Improved mapping of the ocean floor, combined with better seismic imaging of the subsurface, has led to the realisation that significant portions of the continental margins are associated with gravity-driven slumping of unlithified sediments, resulting in mass transport deposits (MTDs) (e.g Scarselli et al., 2016 and references therein). Similar, but as yet largely unrecognised, MTD's may be preserved within the geological record, but their recognition may be hindered by subsequent geological processes and tectonism (see Waldron and Gagnon, 2011). Identification of structures attributable to 'soft-sediment' deformation (SSD) (see Maltman, 1984), rather than 'hard-rock' deformation (HRD) marking subsequent tectonism of lithified successions, can therefore be problematic. It has intrigued geologists for more than a century (e.g. Grabau, 1913, p.660; see Maltman 1994a), and is encapsulated by McCallien (1935, p.426) who notes "the question arises of whether the inversion (of strata) occurred upon the sea bottom or posteriorly during the (regional) folding" (see also Jones, 1939; Woodcock, 1976, 1979; Elliot and Williams, 1988). While the identification of syn-sedimentary extensional 'growth' faults is relatively straightforward, the interpretation of contractional folds and fabrics created while

sediments were unlithified remains more challenging. Indeed, folds created during SSD and HRD may be geometrically indistinguishable from one another. The misidentification of contractional structures formed during SSD may have profound consequences in the interpretation of regional geological histories and is perhaps the most critical relationship to determine with confidence.

Criteria for the recognition of SSD in subsequently lithified rocks have been the focus of a number of publications (e.g. Woodcock, 1976; Elliot and Williams, 1988; McClay, 1991, p.13; Maltman, 1994a, b; Waldron and Gagnon, 2011). However, such criteria have been established either within ancient lithified sequences, with inherent uncertainties as to the true nature of structures, or from drill cores through unlithified successions that offer only a restricted and narrow view of such structures. The late-Pleistocene Lisan Formation was chosen as a case study because it remains poorly lithified, and folds and thrusts developed within it are unequivocally related to SSD associated with downslope movement of MTDs towards the Dead Sea Basin (Alsop and Marco, 2012a) (Fig. 1a,b). We are therefore able to confidently discuss structures associated with contractional SSD that in other areas may have been described in the context of HRD.

While recognising that complications may arise if regional tectonism (rather than gravity-driven deformation) affects unlithified successions (Waldron and Gagnon, 2011; Korneva et al., 2016), this study concentrates on SSD structures that formed during gravity-driven slumping (e.g. Alsop et al., 2017a and references therein). We raise two important research questions that may aid in the interpretation and diagnosis of SSD and HRD in ancient lithified sequences:

i) How do we distinguish folds and fabrics developed during SSD and HRD?

ii) Could SSD fabrics be enhanced during subsequent compaction and diagenesis?

2. Geological Setting

The Dead Sea Basin is a pull-apart basin developed between two left-stepping, parallel fault strands that define the sinistral Dead Sea Fault (Garfunkel, 1981) (Fig. 1a). This fault has been active since the early Miocene (Nuriel et al., 2017) including during deposition of the Lisan Formation in the late Pleistocene (70-15 ka) (Haase-Schramm et al., 2004). The Lisan Formation comprises a succession of alternating aragonite-rich and detrital-rich laminae on a sub-millimetre scale that are interpreted as annual varve-like cycles (Begin et al., 1974). Activity along the Dead Sea Fault has resulted in numerous earthquakes which triggered SSD and slumping of MTDs (e.g. El-Isa and Mustafa, 1986; Marco et al., 1996). The upper part of the Lisan Formation that we examine is less than 40 ka (Haase-Schramm et al., 2004), has never developed a thick (< 10 m) overburden, and remains unlithified to the present day. In fact, the Lisan Formation currently still contains 25% fluid (Arkin and Michaeli, 1986, see also Frydman et al., 2008), and is generally considered to have been fluid-saturated at the time of deformation (e.g. Alsop et al., 2016), meaning that it was susceptible to loss of shear strength and SSD during seismicity (e.g. Maltman, 1994a; Weinberger et al., 2016). Further evidence that the Lisan Formation remained poorly cemented at the time of deformation is provided by analysis of thin sections that reveal a lack of brecciation (Alsop and Marco, 2011). Re-mobilisation of sediments following thrusting (Alsop and Marco, 2011), and injection of numerous clastic dykes that cut the MTD horizons, and are sourced from within the lower portions of Lisan Formation (Levi et al., 2008), also demonstrate that structures within the Lisan Formation were unequivocally created during SSD.

The case study area (N 31º0449.6 E 35º2104.2) is located at Wadi Peratzim on the Am'iaz Plain, which is a down-faulted block directly east of the Dead Sea western border fault zone (Fig. 1b).

3. Observations of structures created during soft-sediment deformation

3.1. Truncation of folds

Individual MTDs within the Lisan Formation are typically <1.5 m thick and are capped by undeformed horizontal beds (Fig. 2a). Upright and recumbent slump folds within the MTDs display truncation of their hinges and limbs (Fig. 2b-e). In some cases, tens of centimetres of stratigraphy have been removed from the upper fold limbs via erosive down-cutting along relatively planar (Fig. 2b,c) or irregular surfaces (Fig. 2d,e) (Alsop and Marco, 2012b). The truncation of folds indicates that they formed prior to erosive down-cutting.

3.2. Sedimentary infilling of erosive surfaces

Erosive surfaces are overlain by sedimentary 'caps' that comprise mud, silt, sand and millimetre-scale aragonite fragments, which infill irregularities and topography along the surface (Fig. 2e-i). Such sedimentary caps, which may be graded, are 2-10 cm thick (and exceptionally up to 30 cm), with sharp irregular bases and planar, horizontal upper surfaces (Fig. 2e-g). Occasionally, topographic highs, created by underlying folds, are overlain by caps and sediments that display drape folding, characterised by thinning over 'highs' and thickening towards underlying 'lows' (Fig. 2e-i). These relationships demonstrate that deformation occurred prior to deposition of the overlying sedimentary caps that are interpreted to be deposited out of suspension following slope failure (Alsop et al., 2016).

3.3. Incorporation of folded sedimentary clasts

Sedimentary caps within the Lisan Formation may incorporate centimetre-scale angular fragments of aragonite laminae that, in some instances, contain pre-existing folds (Fig. 3a). Fragments of folded aragonite were locally formed, reworked and incorporated into sedimentary caps during SSD associated with individual MTD events (Alsop and Marco, 2012b). Fragments containing folds unequivocally demonstrate that deformation occurred prior to incorporation of clasts into the sedimentary cap.

3.4. Cross-cutting clastic dykes

Clastic dykes are created by fluidization and injection of over-pressured sediment along hydraulic fractures during seismic events (Levi et al., 2006; 2008). Within the Lisan Formation, individual clastic dykes are typically <30 cm in width, and may branch and intrude across several different MTDs and undeformed horizons (Fig. 3b,c). Clastic dykes display internal banding that is parallel to the margins of the intrusion and may reflect multiple 'pulses' of flow during injection (Fig. 3c). The sharply cross-cutting nature of clastic dykes provides clear evidence that they were intruded after slumping of MTDs.

3.5. Folding and axial-planar cleavage

Slump folds within the Lisan Formation are defined by thin detrital beds that display a parallel style of folding, together with extreme thickening of weak aragonite-rich beds into fold cores (see Alsop et al. 2017a for details) (Figs. 2b, 3d,e). Competent, thin, detrital beds may also

define classical 'S'- and 'Z'-verging parasitic fold geometries around larger scale folds (Fig. 3d). Axial-planar cleavages and associated intersection lineations have also been described from slump folds of the Lisan Formation (Alsop and Marco, 2014). These include grain-shape fabrics defined by aragonite fragments, together with spaced fracture cleavage (Fig. 3e) and crenulation cleavage (Fig. 3f,g). The cleavage is axial-planar to both recumbent and upright folds which are restricted to MTD horizons. These observations of folds and fabrics demonstrate that, at the time of folding, mud-rich units were locally more competent than the aragonite beds.

3.6. Mineralised cleavage and thrust planes

Within some mud-rich units of the Lisan Formation, the spaced fractures and cleavage associated with slumping is marked by gypsum that has precipitated as ~1 mm thick veins along the cleavage plane (Fig. 3h,i). Gypsum is formed along extensional fractures displaying syn-sedimentary thickening and 'growth' of hangingwall strata (Fig. 3h,i), and also along some of the larger thrust planes defining imbricate systems within the MTDs (Alsop et al., 2017a). The presence of gypsum along cleavages and faults within deformed horizons indicates that it precipitates in unlithified sediments during or very shortly after MTD emplacement.

4. How do we distinguish folds and fabrics developed during SSD and HRD?

4.1. Regional patterns of folds and fabrics

Folds and fabrics generated by SSD within MTDs may define coherent patterns of fold vergence consistent with downslope movement towards the basin depocentre (Fig. 4a.1). Within the Dead Sea Basin, the slump folds of the Lisan Formation define a simple radial pattern of slumping extending for more than 100 km along strike and directed towards the depocentre of the basin (Alsop and Marco, 2012a; Weinberger et al., 2017) (Fig. 1b). If the pattern of fold and fabric vergence can be linked directly to gross basin geometry, then this supports a sedimentary origin. Ideally, a viable mechanism to trigger SSD, such as sediment overloading and/or seismicity, should also be apparent. Both the gross basin geometry and triggering mechanisms may become more difficult to interpret in the ancient rock record where the palaeogeography and tectonic setting are less well-constrained.

Alternatively, if regional contraction is the cause of folds and fabrics during HRD, then there should ideally be abundant evidence of folding and thrusting (that may also involve underlying basement), together with consistent directions of vergence reflecting large-scale tectonic controls (Fig. 4b.1).

4.2. Folds and fabrics are truncated by overlying sequences

Folds and fabrics created during SSD are abruptly truncated by overlying erosive surfaces within the Lisan Formation, (Figs. 2b-f, 4a.2). Erosive truncation of underlying structures demonstrates that they were created at or close to the sediment surface, and were then exposed to surficial processes. In the rock record, a careful distinction needs to be drawn between truncating surfaces that are tectonic detachments, and are typically planar and bedding-parallel (or actually cut up-section) (Fig. 4b.2), versus those of sedimentary origin that are erosive and may be highly irregular and infilled by overlying sediments (Fig. 4b.2). A further caveat in determining SSD is that erosion was 'syn-depositional' with respect to the underlying succession, rather than a potentially much later angular unconformity. Such regional unconformities may be readily

distinguished where they display significant relief and cross-cut several underlying stratigraphic units. In addition, regional unconformities are frequently marked by contrasting sedimentary facies (if not metamorphic grades) in the overlying and underlying sequences. Conversely, truncations associated with SSD are more typically restricted to particular MTD horizons, with sedimentation of similar facies to that incorporated in the MTD simply resuming after the failure event. While MTDs and their associated unconformities are repeatedly developed after each successive failure event, regional unconformities cutting HRD will typically be less frequent and more widely spaced in vertical sections.

4.3. Folds and fabrics are restricted to particular horizons.

SSD is only developed within particular horizons, while intervening beds between these MTDs remain undeformed within the Lisan Formation (Figs. 2a, 4a.3). However, these intervening beds locally thicken to infill deformation-related topography in underlying MTDs (Alsop and Marco, 2013). Although deformation being restricted to a particular horizon has been quoted as a reliable means to separate SSD from tectonic structures, Elliot and Williams (1988) have pointed out that tectonic deformation may itself become restricted along bedding-parallel detachments (Fig. 4b.3). While HRD is perhaps less likely to be restricted to particular stratigraphic horizons, and will be prone to migrate up or down section when traced laterally, the key criterion in distinguishing SSD and HRD is that sediment infills topography along the irregular top surface of MTDs.

4.4. Folds and fabrics are incorporated into overlying horizons.

Folded aragonite layers may become detached and incorporated into the detrital capping layer that is deposited above erosive unconformities (Figs. 3a, 4a.4). The relatively large size (up to 10 cm long) of some folded clasts, coupled with their broken and disaggregated appearance, suggests that they were fragile and could not have survived transportation over long distances. The implication is that the folded fragments were derived from the immediately underlying MTD. Such relationships could not be created during HRD unless a significant unconformity existed along the top of a deformed succession, and this should be distinguishable by its greater extent and potential to cut more deeply across underlying sequences. While basal conglomerates overlying regional unconformities may contain fragments of underlying folded lithologies created during HRD (Fig. 4b.4), the incorporation of folded clasts that can be shown to have been fragile and disaggregating at the time of deposition is distinctive of MTDs. In addition, regional unconformities transecting underlying HRD structures may contain rounded clasts of ‘exotic’ lithologies that are less likely within sedimentary caps marking SSD (Fig. 4b.4).

4.5. Folds and fabrics are cut by clastic dykes.

If folds and fabrics are cut by injected clastic dykes (e.g. Figs. 3b, 4a.5), then this provides clear evidence that these structures were formed by SSD during deposition of the succession rather than by a later HRD event. However, care must be taken when interpreting clastic dykes to ensure that sediment is injected, rather than ‘neptunian’ where sediment may simply fall in and fill an existing open fissure within lithified rocks (Fig. 4b.5). Such neptunian infills may be marked by horizontal stratification, reflecting successive infill events, whereas injected clastic dykes may display internal flow banding parallel to the dyke margins (Figs. 3c, 4a.5). In

addition, linking of clastic dykes directly into underlying source layers also provides evidence for the injection of sediment. Finally, caution should be exercised as clastic dykes can inject during regional contraction, and thereby potentially cut folds related to HRD (e.g. Palladino et al., 2016).

4.6. Fold style and axial-planar fabrics.

During SSD, unlithified muds may undergo buckle folding and appear more competent than adjacent sands, principally due to the greater porosity of sand allowing more water to be retained thereby reducing shear strength (Fig. 4a.6) (see Waldron and Gagnon, 2011). Conversely, lithified sandstones are generally more competent than adjacent mudstones during HRD (Fig. 4b.6). Within the case study, some thin mud layers display buckle fold geometries suggesting they are more competent than the surrounding aragonite-rich horizons (Figs. 2b, 3d, 4a.6). Although it has previously been suggested by Alsop and Marco (2013, p.66) that folds formed during SSD do not develop parasitic fold hinges, we now recognise thin detrital-rich horizons defining trains of buckle folds that switch vergence as the layer is traced around higher-order fold hinges (Figs. 3d, 4a.6). The presence or absence of parasitic 'S' and 'Z' folds should not therefore be used as a discriminator of the SSD or HRD origin of folds.

While the potential relationship of sedimentary fabrics to the axial planes of slump folds has been previously debated (e.g. Elliot and Williams, 1988; McClay, 1991; Maltman, 1994b), it has now been shown that folds created by SSD within the Lisan Formation display a range of axial-planar grain-shape, crenulation and fracture cleavages (Figs. 3d-f, 4a.6) (Alsop and Marco, 2014; Weinberger et al., 2017). Crenulation cleavage is created by microfolding of the millimetre-scale aragonite- and detrital- rich laminae, while fracture cleavage is associated with shear and displacement of laminae (see Alsop and Marco, 2014 for further details) (Fig. 3e-g). Thin section analysis of crenulation hinges and axial planar fractures from the Lisan Formation was presented by Alsop and Marco (2014, their fig. 3) and reveals no evidence of pressure solution or solution mass transfer, with fractures being perfectly sharp and lacking any trace of insoluble residue along them. The cleavages observed from the Lisan Formation were therefore created during SSD, and similar fabrics have also been recorded from deeper-water siliclastic sediments in older (Carboniferous) sequences (e.g. Strachan and Alsop 2006, p.460; Sobiesiak et al. 2017, p.184). We emphasise that the presence or absence of axial-planar fabrics cannot therefore be used to distinguish folds created during HRD or SSD across a range of lithologies and settings.

4.7. Folds and fabrics are mineralised.

Although thin gypsum veins are developed along fabrics and syn-sedimentary faults within the Lisan Formation (Figs. 3h,i, 4a.7), mineralisation is more typically considered to be restricted to tectonic faults linked to HRD (Fig. 4b.7) (McClay, 1991, p.14). Indeed, Elliot and Williams (1988, p.181) note that brittle structures "locally contain vein filling of secondary minerals, which indicates that lithification was advanced before deformation" and "this is not to be expected in the near-surface deformation of sediments". This view has however been questioned by Maltman (1994b, p.304) who cites examples of mineralisation associated with SSD. Our observation that thin gypsum veins form along fabrics (Figs. 3h,i, 4a.7) shows that the presence of mineralised cleavage planes is insufficient evidence to categorically demonstrate that cleavage

was formed by HRD. Although precipitation of gypsum along fabrics (and for that matter thrust planes) could arguably be slightly later, the observation that gypsum has formed along, and is restricted to such fabrics and faults within individual MTDs, suggests that gypsum precipitated during (and shortly after) SSD. We therefore contend that the presence or absence of mineralisation cannot be used to differentiate structures formed during HRD from those created via SSD.

5. Could SSD fabrics be enhanced during subsequent compaction and diagenesis?

Farrell and Eaton (1988) suggest that the two main processes responsible for forming or modifying SSD fabrics are liquidization and compaction. There is, however, no evidence within the Lisan Formation that liquidization (where grains undergo particulate flow) has played a major role as millimetre-scale laminae remain intact despite the development of fold-related fabrics (see Alsop and Marco, 2014). Compaction is created by overburden imparting a pure strain, resulting in vertical shortening and enhancement of sub-horizontal fabrics created during SSD (Farrell and Eaton, 1988). It has also been suggested by Maltman (1981) that with increasing depth of burial, diagenesis may 'lock-in' primary sedimentary fabrics related to settling or compaction of grains. Growth of any new mineral phases during diagenesis may be controlled by the orientation of this existing sedimentary fabric (Maltman, 1981). A number of criteria may help determine if the origin of a fabric is linked to subsequent compaction and diagenesis of MTD's in the rock record.

5.1. Thickness of overburden.

Maltman (1981) suggests that the presence of interstitial water reduces intergranular friction thereby encouraging rotation of grains to create bedding-parallel compaction fabrics. This will occur "early in the history of the sediment, possibly within the first few metres of burial" (Maltman, 1981, p.476). This interpretation has however been subsequently questioned by Elliot and Williams (1988, p.174) who note that deformation fabrics are not preserved in drill core samples from modern sediment that is shallower than 100 m below the sea bed. Although the upper part of the Lisan Formation has never had a significant (typically <10 m) overburden, this could still be sufficient to generate compaction-related fabrics in some cases. Indeed, the palaeomagnetic inclination record from the Lisan Formation is interpreted to show a shallowing effect possibly linked to compaction (Marco et al., 1998). Thus, a degree of ambiguity remains as to the amount of overburden required to generate compaction fabrics in unconsolidated sediment, and limited overburden cannot be used as a basis to discount such fabrics.

5.2. Distribution and orientation of folds and fabrics.

As compaction post-dates the MTD event and is incrementally built up as overlying sediments are deposited, it should broadly affect both the buried MTD horizons and intervening non-deformed units equally. It is therefore notable that within the case study, fabrics are not observed in the undeformed beds between individual MTDs. Within the Lisan Formation, the relatively weak and open nature of late-stage folds and fabrics previously attributed to compaction suggests its effects are also limited within MTDs (Alsop et al., 2016). Thrust faults and normal faults generated during slumping in the study area maintain classical dip angles of 30° and 60°

respectively (Alsop et al., 2017b). This indicates that they have not undergone significant flattening during any subsequent compaction.

As compaction is a gravity-driven process, resulting fabrics are typically considered to be uniformly orientated and sub-horizontal. However, cleavage within the case study is variably dipping and fans around recumbent slump folds. Within a number of folds, the syn-slumping spaced cleavage also displays systematic kinematic reversals when traced around folds that are consistent with a flexural shear mechanism (Alsop and Marco, 2014). Sub-horizontal compaction or mimetic fabrics that fortuitously become axial-planar to recumbent slump folds would not be expected to display any such kinematic variation around the fold hinge as a) there is no genetic relationship between the fold and subsequent fabric, and b) offset across the cleavage planes would not occur following mimetic growth of minerals. Multiple sets of variably orientated cleavage, combined with kinematic reversals around fold hinges, are inconsistent with compaction or mimetic growth of fabrics.

5.3. Deformation of vertical markers.

Clastic dykes can act as markers to calculate the amount of vertical shortening associated with compaction. Based on folding of vertical clastic dykes, Smith (2000) calculated that there may be up to 30% compaction in some cases. Care should be taken as clastic dykes intruded within contractional settings may themselves be folded by tectonics rather than compaction (e.g. Palladino et al., 2016). Within the case study, vertical clastic dykes that cross-cut the MTDs preserve their original injection fabrics (e.g. Levi et al., 2006), and do not display any evidence of buckling linked to vertical compaction of the succession (Fig. 3b,c).

6. Conclusions

Folds and fabrics developed in the late-Pleistocene Lisan Formation were indisputably created via SSD during slumping of MTDs towards the Dead Sea Basin. Our observations are therefore directly relevant to the debate spanning over a century regarding the value of folds and fabrics in distinguishing SSD and HRD. We demonstrate that a range of criteria, including the restriction of folds and fabrics to within discrete horizons, their truncation by overlying erosive surfaces, the incorporation of fragile, folded clasts into sedimentary caps, the presence of vertical clastic dykes that injected across folds and fabrics, and vergence of folds towards the sedimentary depocentre, are all valuable tools when discriminating structures created during SSD and HRD. The style of folding in different lithologies, especially where mud is shown to be more competent than sand (Waldron and Gagnon, 2011), is also a key criterion when distinguishing folds created during SSD from those formed during HRD. Axial-planar fabrics are developed around folds within MTDs, and we conclude that such fabrics may not therefore be used to differentiate folds created during SSD or HRD. In addition, we show that mineralised (gypsum-filled) fractures and cleavages develop during SSD and cannot be considered diagnostic of HRD. The range of observations and evidence discussed above collectively leads us to conclude that compaction and diagenesis have not played a significant role in the modification of folds and fabrics in the case study. However, more general caution should be exercised as compaction and diagenesis have the potential to considerably enhance and alter folds and fabrics originally created by SSD and now preserved in the rock record where significant overburdens exist.

Continuing improvements in seismic resolution, as witnessed over the past 40 years, will help drive further understanding of structural and stratigraphic detail around modern MTDs, and this knowledge may ultimately aid in the recognition of large-scale SSD in the rock record. The single most useful criterion to distinguish structures formed during SSD are irregular erosive surfaces that truncate underlying structures and are themselves overlain and infilled by sedimentary caps and stratigraphy. This infilling 'sedimentary fingerprint' that thins across underlying structural highs, at the scale of the outcrop or seismic section, provides the most compelling evidence for a SSD origin. However, even in this situation care must be taken in the rock record that the erosive surface is not a subsequent regional unconformity.

Acknowledgements

SM acknowledges the Israel Science Foundation (ISF grant No. 1436/14) and the Ministry of National Infrastructures, Energy and Water Resources (grant #214-17-027). RW was supported by the Israel Science Foundation (ISF grant No. 868/17). We thank John Waldron and Nigel Woodcock for providing detailed reviews that improved the manuscript, together with Toru Takeshita for careful editorial handling.

Fig. 1 a). General map showing tectonic plates in the Middle East and the location of the Dead Sea Fault (DSF). b) Map of the Dead Sea showing the position of the study area, and mass transport deposit (MTD) slump directions (arrows).

Fig. 2. Photographs from the Peratzim area of (a-c) truncated slump folds and (d-g) overlying sedimentary caps (denoted by double-headed arrows) that thin across (h-i) underlying structural 'highs'. Scale is provided by a 10 cm chequered rule.

Fig. 3. Photographs from the Peratzim area of a) folded aragonite fragments, b, c) injected clastic dykes, d) 'S' and 'Z' minor buckle folds. e) Spaced fracture cleavage and, f, g) crenulation cleavage that are axial-planar to slump folds. h, i) show extensional fractures marked by gypsum veining. Scale is provided by a 10 cm chequered rule and a 15 mm diameter coin.

Fig. 4. Schematic cartoons summarising fold and fabric relationships linked to (a) soft-sediment deformation (SSD) in mass transport deposits (MTD), and (b) regional tectonics in hard-rock deformation (HRD). In a), more competent beds during SSD (such as detrital muds) are shown in brown, whereas in b) units behaving relatively competently during HRD are highlighted in yellow. In each case, basal detachments (BD) are highlighted in red, and unconformities (U/C) in blue. Circled numbers (1, 2 etc.) refer to specific relationships discussed in the text (Fig. 4a.1, 4b.2 etc.).

References

Alsop, G.I., Marco, S. 2011. Soft-sediment deformation within seismogenic slumps of the Dead Sea Basin. *Journal of Structural Geology* 33, 433-457.

Alsop, G.I., Marco, S. 2012a. A large-scale radial pattern of seismogenic slumping towards the Dead Sea Basin. *Journal of the Geological Society* 169, 99-110.

Alsop, G.I., Marco, S. 2012b. Tsunami and seiche-triggered deformation within offshore sediments. *Sedimentary Geology* 261, 90-107.

Alsop, G.I., Marco, S. 2013. Seismogenic slump folds formed by gravity-driven tectonics down a negligible subaqueous slope. *Tectonophysics* 605, 48-69.

Alsop, G.I., Marco, S. 2014. Fold and fabric relationships in temporally and spatially evolving slump systems: A multi-cell flow model. *Journal of Structural Geology*, 63, 27-49.

396 Alsop, G.I., Marco, S., Weinberger, R., Levi, T. 2016. Sedimentary and structural controls on
397 seismogenic slumping within Mass Transport Deposits from the Dead Sea Basin. Sedimentary Geology
398 344, 71-90.
399 Alsop, G.I., Marco, S., Levi, T., Weinberger, R. 2017a. Fold and thrust systems in Mass Transport
400 Deposits. Journal of Structural Geology 94, 98-115.
401 Alsop, G.I., Marco, S., Weinberger, R., Levi, T. 2017b. Upslope-verging back thrusts developed during
402 downslope-directed slumping of mass transport deposits. Journal of Structural Geology 100, 45-61.
403 Arkin, Y., Michaeli, L. 1986. The significance of shear strength in the deformation of laminated
404 sediments in the Dead Sea area. Israel Journal of Earth Sciences 35, 61-72.
405 Begin, Z.B., Ehrlich, A., and Nathan, Y., 1974, Lake Lisan, the Pleistocene precursor of the Dead Sea:
406 Geol. Surv. Isr. Bull., v. 63, p. 30.
407 Elliot, C.G. & Williams, P.F. 1988. Sediment slump structures: A review of diagnostic criteria and
408 application to an example from Newfoundland. Journal of Structural Geology 10, 171-182.
409 El-Isa, Z.H., and Mustafa, H., 1986, Earthquake deformations in the Lisan deposits and seismotectonic
410 implications: Geophys. J. R. Astron. Soc., v. 86, p. 413-424.
411 Farrell, S.G., Eaton, S. 1988. Foliations developed during slump deformation of Miocene marine
412 sediments, Cyprus. Journal of Structural Geology 10, 567-576.
413 Frydman, S., Charrach, J., Goretsky, I. 2008. Geotechnical properties of evaporite soils of the Dead Sea
414 area. Engineering Geology101, 236-244.
415 Garfunkel, Z., 1981, Internal structure of the Dead Sea leaky transform (rift) in relation to plate
416 kinematics: Tectonophysics, v. 80, p. 81-108.
417 Grabau, A.W. 1913. Principles of stratigraphy. A.G. Seiler and Co., New York, 1185 pp.
418 Haase-Schramm, A., Goldstein, S.L., Stein, M. 2004. U-Th dating of Lake Lisan aragonite (late
419 Pleistocene Dead Sea) and implications for glacial East Mediterranean climate change. Geochimica et
420 Cosmochimica Acta 68, 985-1005.
421 Jones, O.T. 1939. The geology of the Colwyn bay district: a study of submarine slumping during the
422 Salopian period. *Q. J. Geol. Soc. London*, 380, 335-382.
423 Korneva, I., Tondi, E., Jablonska, D., Di Celma, C., Alsop, I., Agosta, F. 2016. Distinguishing
424 tectonically-and gravity-driven synsedimentary deformation structures along the Apulian platform margin
425 (Gargano Promontory, southern Italy). Marine and Petroleum Geology73, 479-491.
426 Levi, T., Weinberger, R., Aïfa, T., Eyal, Y., Marco, S., 2006. Injection mechanism of clay-rich sediments
427 into dikes during earthquakes: Geochemistry, Geophysics, and Geosystems, v. 7, no. 12, p. Q12009
428 Levi, T., Weinberger, R., Eyal, Y., Lyakhovsky, V., Heifetz, E. 2008. Velocities and driving pressures of
429 clay-rich sediments injected into clastic dykes during earthquakes. Geophysical Journal International
430 175, 1095-1107.
431 Maltman, A. 1981. Primary bedding-parallel fabrics in structural geology. Journal of the Geological
432 society, London 138, 475-483.
433 Maltman, A. 1984. On the term soft-sediment deformation. Journal of Structural Geology 6, 589-592.
434 Maltman, A. 1994a. Introduction and Overview. In: Maltman, A. (Editor) The Geological Deformation of
435 Sediments. Chapman & Hall, London. pp. 1-35.
436 Maltman, A. 1994b. Deformation structures preserved in rocks. In: Maltman, A. (Editor) The Geological
437 Deformation of Sediments. Chapman & Hall, London. pp. 261-307.
438 McCallien, W.J. 1935. The metamorphic rocks of Inishowen, Co. Donegal. Proceedings of the Royal Irish
439 Academy, 42B, 407-442.
440 McClay, K.R. 1991. The mapping of geological structures. John Wiley & Sons, Chichester, 168pp.
441 Marco, S., Stein, M., Agnon, A., and Ron, H., 1996, Long term earthquake clustering: a 50,000 year
442 paleoseismic record in the Dead Sea Graben: J. Geophys. Res., v. 101, p. 6179-6192.
443 Marco, S., Ron, H., McWilliams, M.O., Stein, M. 1998. High-resolution record of geomagnetic secular
444 variation from Late Pleistocene Lake Lisan sediments (palaeo Dead Sea). Earth and Planetary Science
445 Letters 161, 145-160.
446 Nuriel,P., Weinberger, R., Kylander-Clark, A.R.C., Hacker, B.R., Cradock, J.P. 2017. The onset of the
447 Dead Sea transform based on calcite age-strain analyses. Geology 45, 587-590.
448 Palladino, G., Grippa, A., Bureau, D., Alsop, G.I., Hurst, A. 2016. Emplacement of sandstone intrusions
449 during contractional tectonics. Journal of Structural Geology 89, 239-249.

Scarselli, N., McClay, K., Elders, C. 2016. Seismic geomorphology of Cretaceous megaslides offshore Namibia (Orange Basin): Insights into segmentation and degradation of gravity-driven linked systems. Marine and Petroleum Geology 75, 151-180.

Smith, J.V. 2000. Flow pattern within a Permian submarine slump recorded by oblique folds and deformed fossils, Ulladulla, south-eastern Australia. *Sedimentology*, 47, 357-366.

Sobiesiak, M.S., Alsop, G.I., Kneller, B., Milana, J-P. 2017. Sub-seismic scale folding and thrusting within an exposed mass transport deposit: A case study from NW Argentina. Journal of Structural Geology 96, 176-191.

Strachan, L.J., Alsop, G.I. 2006. Slump folds as estimators of palaeoslope: a case study from the Fisherstreet Slump of County Clare, Ireland. Basin Research 18, 451-470.

Waldron, J.W.F., Gagnon, J-F. 2011. Recognizing soft-sediment structures in deformed rocks of orogens. Journal of Structural Geology 33, 271-279.

Weinberger, R., Levi, T., Alsop, G.I., Eyal, Y. 2016. Coseismic horizontal slip revealed by sheared clastic dikes in the Dead Sea basin. Geological Society of America Bulletin 128, 1193-1206.

Weinberger, R., Levi, T., Alsop, G.I., Marco, S. 2017. Kinematics of Mass Transport Deposits revealed by magnetic fabrics. Geophysical Research Letters, 44, doi: 10.1002/2017GL074471.

Woodcock, N. H 1976. Structural style in slump sheets: Ludlow Series, Powys, Wales. Journal of the Geological Society, London 132, 399-415.

Woodcock, N.H. 1979. Sizes of submarine slides and their significance. Journal of Structural geology, 1, 137-142.

Figure 1

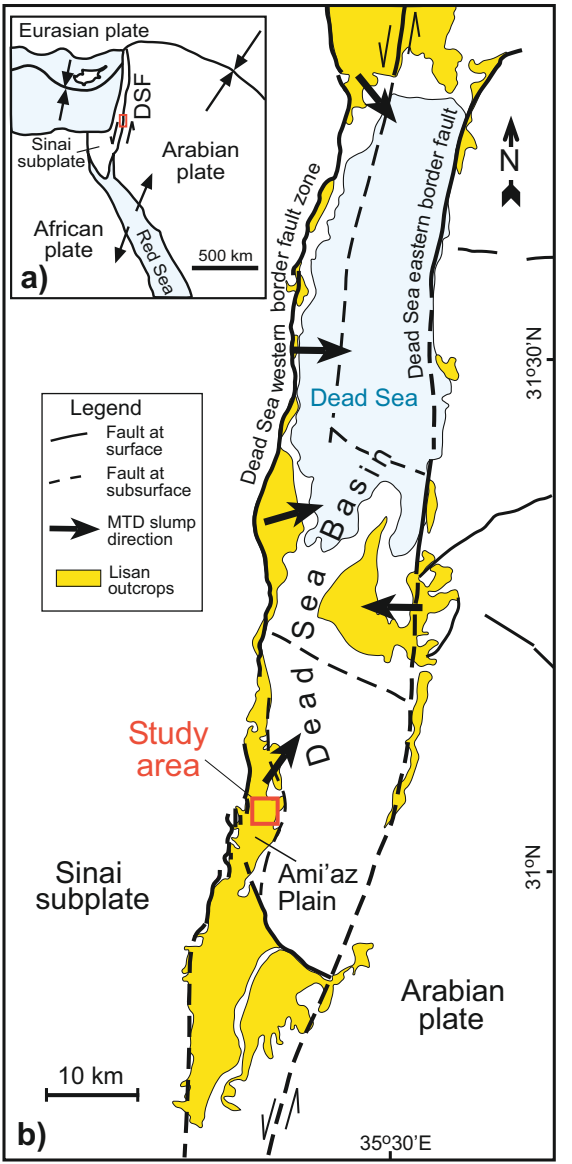
Eurasian plate
DSF
Sinai subplate
Arabian plate
African plate
Red Sea
500 km
a)
Legend
Fault at surface
Fault at subsurface
MTD slump direction
Lisan outcrops
Dead Sea western border fault zone
Dead Sea eastern border fault
Dead Sea
Dead Sea Basin
N
31°30'N
31°N
Study area
Sinai subplate
Ami'az Plain
Arabian plate
10 km
b)
35°30'E

Figure 2

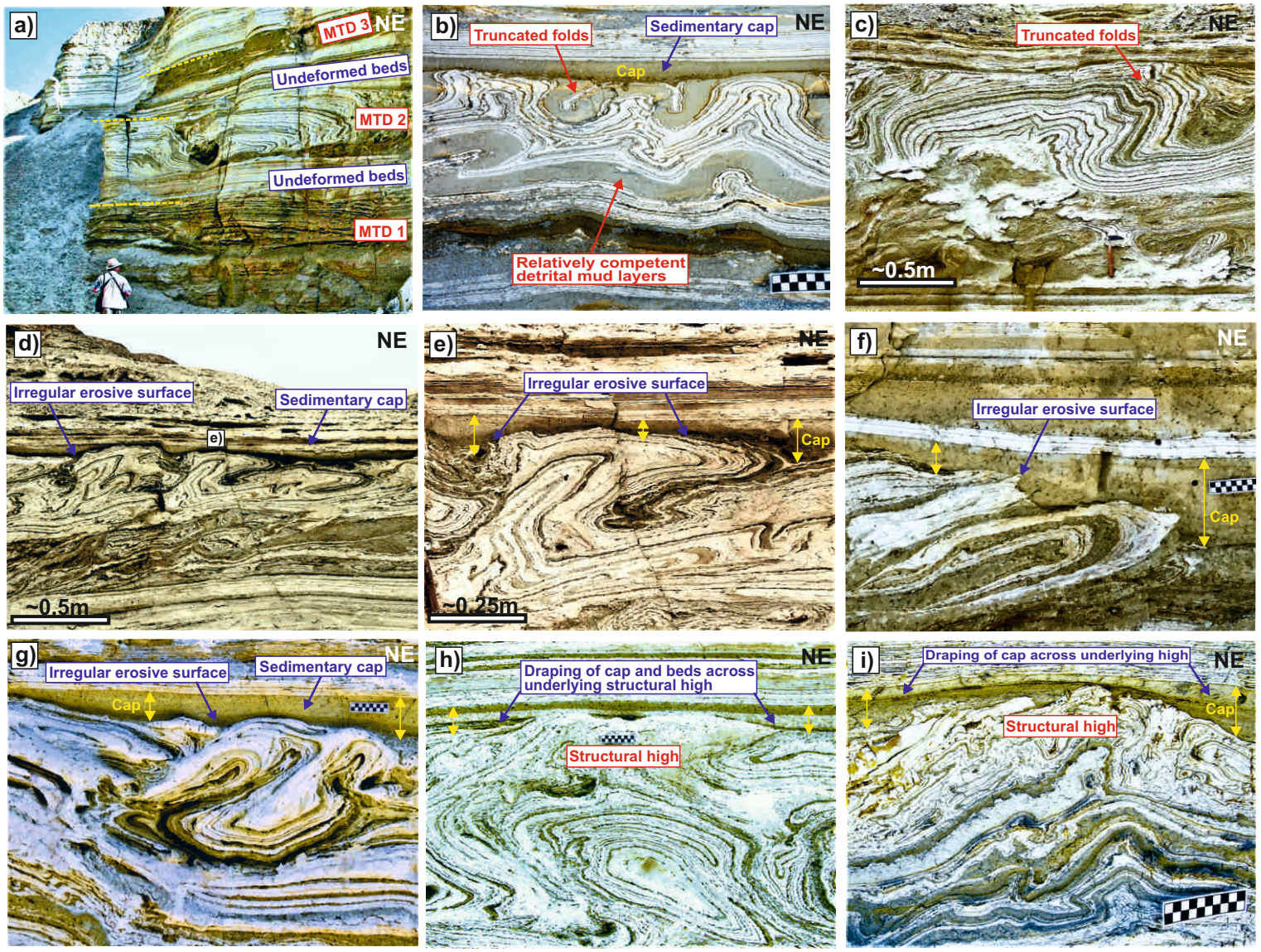
a)
MTD 3
NE
Undeformed beds
MTD 2
Undeformed beds
MTD 1
b)
Truncated folds
Sedimentary cap
NE
Cap
Relatively competent detrital mud layers
c)
Truncated folds
NE
~0.5m
d)
NE
Irregular erosive surface
Sedimentary cap
e)
~0.5m
e)
NE
Irregular erosive surface
Cap
~0.25m
f)
NE
Irregular erosive surface
Cap
g)
Irregular erosive surface
Sedimentary cap
NE
Cap
h)
Draping of cap and beds across underlying structural high
NE
Structural high
i)
Draping of cap across underlying high
NE
Cap
Structural high

Figure 3

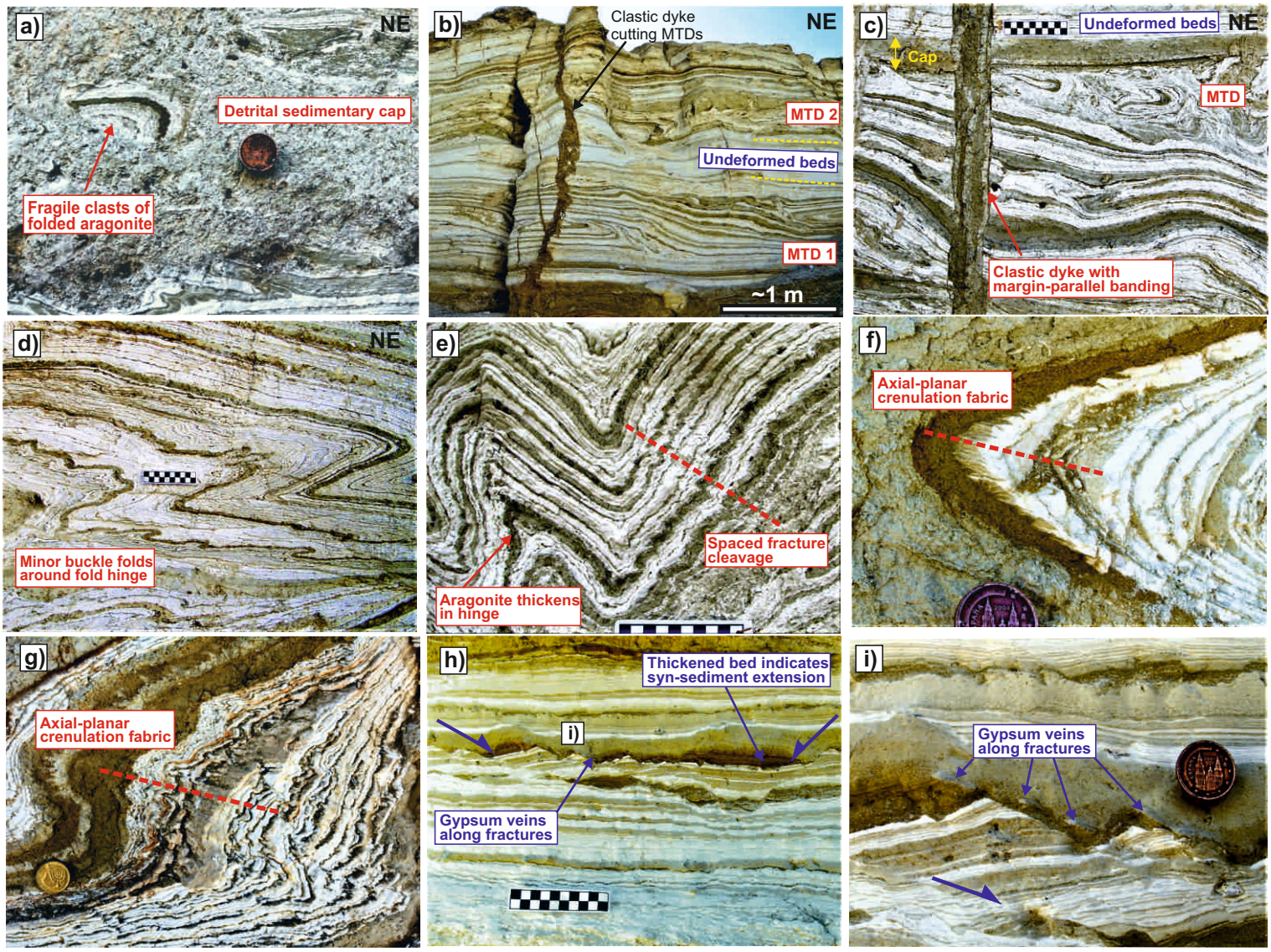
a)
NE
Detrital sedimentary cap
Fragile clasts of folded aragonite
b)
Clastic dyke cutting MTDs
NE
MTD 2
Undeformed beds
MTD 1
~1 m
c)
Undeformed beds
NE
Cap
MTD
Clastic dyke with margin-parallel banding
d)
NE
Minor buckle folds around fold hinge
e)
Spaced fracture cleavage
Aragonite thickens in hinge
f)
Axial-planar crenulation fabric
g)
Axial-planar crenulation fabric
h)
Thickened bed indicates syn-sediment extension
i)
Gypsum veins along fractures
i)
Gypsum veins along fractures

Figure 4

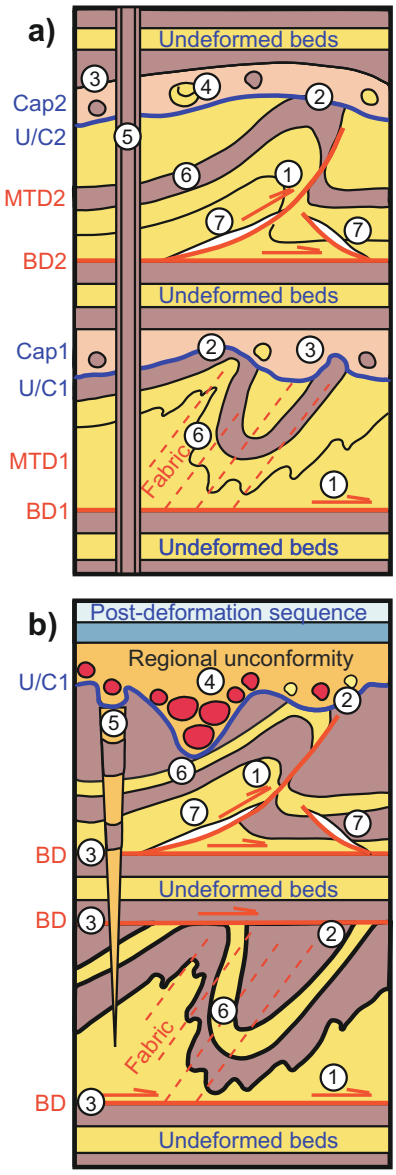
a)
Undeformed beds
Cap2
U/C2
MTD2
BD2
Undeformed beds
Cap1
U/C1
MTD1
BD1
Fabric
Undeformed beds
b)
Post-deformation sequence
Regional unconformity
U/C1
BD
Undeformed beds
BD
Fabric
BD
Undeformed beds